

See discussions, stats, and author profiles for this publication at: <https://www.researchgate.net/publication/269636006>

# An adaptive selective frequency damping method

Article in *Physics of Fluids* · September 2015

DOI: 10.1063/1.4932107

---

CITATIONS

44

---

READS

533

3 authors, including:



**Bastien E. Jordi**

Imperial College London

5 PUBLICATIONS 715 CITATIONS

[SEE PROFILE](#)



**Spencer J. Sherwin**

Imperial College London

437 PUBLICATIONS 16,906 CITATIONS

[SEE PROFILE](#)

# Encapsulated formulation of the Selective Frequency Damping method

Bastien E. Jordi,<sup>1, a)</sup> Colin J. Cotter,<sup>2</sup> and Spencer J. Sherwin<sup>1</sup>

<sup>1)</sup>Department of Aeronautics, Imperial College, London SW7 2AZ, United Kingdom

<sup>2)</sup>Department of Mathematics, Imperial College, London SW7 2AZ, United Kingdom

(Dated: 9 October 2014)

We present an alternative “encapsulated” formulation of the Selective Frequency Damping method for finding unstable equilibria of dynamical systems, which is particularly useful when analysing the stability of fluid flows. The formulation makes use of splitting methods, which means that it can be wrapped around an existing time-stepping code as a “black box”. The method is first applied to a scalar problem in order to analyse its stability and highlight the roles of the control coefficient  $\chi$  and the filter width  $\Delta$  in the convergence (or not) towards the steady-state. Then the steady-state of the incompressible flow past a two-dimensional cylinder at  $Re = 100$ , obtained with a code which implements the spectral/ $hp$  element method, is presented.

Keywords: Selective frequency damping, steady-state solver, stability analysis.

## I. INTRODUCTION

Flow stability theory is a major research interest in fluid dynamics. A stability analysis of a flow can help to predict when instabilities arise, and can be used to design flow controllers. To perform a stability analysis, it is necessary to construct the “base flow” around which the system will be linearised. This leads to the challenge of obtaining a steady-state solution of the Navier-Stokes equations, which is particularly interesting when separated flows are studied. There are alternatives to this, namely to compute the time average of an unsteady solution, or to obtain a solution of the Reynolds averaged Navier-Stokes (RANS) equations to use as the base flow. However, these solutions often produce stability properties which are not relevant to the physical solution<sup>1</sup>. Hence, we are interested in solver algorithms to obtain genuine steady-state solutions of the Navier-Stokes equations. One possible approach is to use Newton’s method, because the (quadratic) convergence towards the steady-state is guaranteed if a good initial guess of the solution is used. For challenging flow problems at high Reynolds number, it may be the case that many complicated bifurcations at various Reynolds numbers must be crossed before finding the required solution. Then the Newton’s method must be coupled with a continuation method. As an alternative, Åkervik *et al.*<sup>2</sup> presented a modification of the time-dependent dynamical system, called Selective Frequency Damping (SFD), which tries to reach the steady-state of an unsteady system by damping unstable temporal frequencies. Since it is easy to implement into an existing code, and does not need a good initial guess, this method appeared to be an efficient alternative to classical Newton’s methods. The SFD method has been successfully applied to find steady-solutions of the Navier-Stokes equations, which were then used as a base flow to study stability properties of flows such as the wake of a sphere<sup>3</sup>, a jet in a crossflow<sup>4</sup> or a cavity

flow<sup>5</sup>. However Jones and Sandberg<sup>6</sup> failed to find the steady-state of the compressible flow around a NACA-0012 airfoil at  $Re = 1 \times 10^6$  using the SFD method. It was assumed there that the method was not able to suppress the instabilities present at this Reynolds number without requiring a large damping coefficient and hence impractically long time-integration to converge. Vyazmina<sup>7</sup> studied swirling flows and it was noticed that the SFD method did not converge towards the steady-state when the problem considered had real unstable eigenvalues.

In this paper we present a time discrete formulation of the SFD method which is implemented as a wrapper around an existing “black box” unsteady solver. In section II we first recall the original form of the SFD method and then show that with the splitting methods framework the method can be reformulated. This alternative formulation encapsulates the existing solver. This scheme is applied to a simple one-dimensional problem in section III. The convergence properties of this formulation are studied in order to provide information about the influence of the filter width and the control coefficient on the stability of the method. Then the results obtained by the application of the encapsulated SFD method to a high-order incompressible Navier-Stokes solver are presented in section IV. Finally, we introduce the idea that isolating the most unstable eigenmode of a flow problem and treating it as a one-dimensional problem can give sufficient information in order to ensure the convergence of the SFD problem applied to a Navier-Stokes solver.

## II. PROBLEM FORMULATION

We first recall the basis of the SFD method as it was originally introduced. Then we present the discretized encapsulated formulation.

With appropriate initial and boundary conditions, any system can be written

$$\dot{q} = f(q), \quad (1)$$

where  $q$  represents the problem unknown(s), the dot represents the time derivative and  $f$  is an operator (which

---

<sup>a)</sup>Electronic mail: b.jordi11@imperial.ac.uk

can be nonlinear). The steady-state  $q_s$  of this problem is reached when  $\dot{q}_s = f(q_s) = 0$ .

The main idea of the SFD method is to introduce a linear forcing term on the right-hand side of (1). This term must contain a control coefficient and a target towards which the solution will be driven to. A new problem formulation is then defined such as

$$\dot{q} = f(q) - \chi(q - q_s), \quad (2)$$

where  $\chi$  is the control coefficient and  $q_s$  is the target steady-state. This stabilization technique is called proportional feedback control and is commonly used in control theory<sup>8</sup>. When  $q_s$  is a genuine steady-state, *i.e.*,  $f(q_s) = 0$ , the steady solution of (2) is clearly also the steady solution of (1). However, in practice, especially for real flow problems, the steady-state is generally not known *a priori*. The SFD method addresses this by replacing  $q_s$  by a low-pass filtered version of  $q$ , denoted  $\bar{q}$ . By damping the most dangerous frequencies, the corresponding instabilities are extinguished<sup>2</sup>. This idea was originally introduced by Pruett *et al.*<sup>9,10</sup> in their work on a temporal filtered model developed for large-eddy simulations.

The transfer-function of the first order low-pass time filter used for the SFD method is

$$\frac{\bar{q}}{q} = 1 \times \frac{1}{1 + i\omega\Delta}, \quad (3)$$

where  $\bar{q}$  is the temporally filtered quantity and  $\Delta$  is the filter width. The differential form of this filter is

$$\dot{\bar{q}} = \frac{q - \bar{q}}{\Delta}. \quad (4)$$

This equation can be advanced in time using any appropriate integration scheme.

Considering (2), with the new target solution  $\bar{q}$ , and the filter (4), we obtain the system

$$\begin{cases} \dot{q} = f(q) - \chi(q - \bar{q}), \\ \dot{\bar{q}} = \frac{q - \bar{q}}{\Delta}. \end{cases} \quad (5)$$

This system is the continuous time formulation of the SFD method, as it was first introduced<sup>2</sup>. The filtered solution  $\bar{q}$  is time varying, and the steady-state is reached when  $q = \bar{q}$ . We now present a time-discrete implementation of the SFD method which allows us to wrap code around an existing time-stepping scheme for equation (1). This notion can be linked to Tuckerman's work<sup>11</sup> on the adaptation of time-stepping codes to carry out efficient bifurcation analysis.

System (5) can be discretised within the framework of sequential operator-splitting methods<sup>12</sup>. The system is divided into two smaller subsystems which are solved separately using different numerical schemes. The first subproblem (which can be nonlinear) is simply (1). We introduce the function  $\Phi$  such that the numerical (or exact) solution of (1) at the step  $(n + 1)$  is given by

$$q^{n+1} = \Phi(q^n). \quad (6)$$

The second subproblem is linear and represents the actions of the feedback control and the low-pass time filter. It can be formulated

$$\begin{cases} \dot{q} = -\chi(q - \bar{q}) \\ \dot{\bar{q}} = \frac{q - \bar{q}}{\Delta} \end{cases} \Leftrightarrow \begin{pmatrix} \dot{q} \\ \dot{\bar{q}} \end{pmatrix} = \begin{pmatrix} -\chi I & \chi I \\ I/\Delta & -I/\Delta \end{pmatrix} \begin{pmatrix} q \\ \bar{q} \end{pmatrix}, \quad (7)$$

where  $I$  is the identity matrix. The linear operator defined by (7) will be denoted  $\mathcal{L}$ . This equation can be solved exactly on  $[t^n, t^n + \Delta t]$  and the solution is given by

$$\begin{pmatrix} q(t^{n+1}) \\ \bar{q}(t^{n+1}) \end{pmatrix} = e^{\mathcal{L}\Delta t} \begin{pmatrix} q(t^n) \\ \bar{q}(t^n) \end{pmatrix}, \quad (8)$$

where the expanded expression of  $e^{\mathcal{L}\Delta t}$  is

$$e^{\mathcal{L}\Delta t} = \frac{1}{1 + \chi\Delta} \times \begin{pmatrix} I + \chi\Delta I e^{-(\chi + \frac{1}{\Delta})\Delta t} & \chi\Delta I [1 - e^{-(\chi + \frac{1}{\Delta})\Delta t}] \\ I - I e^{-(\chi + \frac{1}{\Delta})\Delta t} & \chi\Delta I + I e^{-(\chi + \frac{1}{\Delta})\Delta t} \end{pmatrix}. \quad (9)$$

In the construction of a splitting method, the final solution of one subproblem is used as initial condition of the other one. As (6) does not affect  $\bar{q}$ , the discrete formulation of (5) using a first order splitting method is given by

$$\begin{pmatrix} q^{n+1} \\ \bar{q}^{n+1} \end{pmatrix} = e^{\mathcal{L}\Delta t} \begin{pmatrix} \Phi(q^n) \\ \bar{q}^n \end{pmatrix}, \quad (10)$$

where  $\Delta t$  is the time step used within the solver  $\Phi$ . We call this scheme “encapsulated” since  $\Phi$  is not modified but simply used as an input of the linear solver (8). Hence  $\Phi$  can be treated as a “black box”. Codes which solve the Navier-Stokes equations are usually very complicated. If the original problem (1) is a flow problem, implementing an efficient steady-state solver with minimum programming effort can be highly valuable. To implement (10) in an existing code, the only work required is to create an auxiliary variable  $q^*$  which takes the value of the outcome of (6). Then the linear operator  $e^{\mathcal{L}\Delta t}$  (which is constant through time) simply has to be applied to the vector  $(q^*, \bar{q}^n)^T$ .

This method does not converge to a steady-state for arbitrary control coefficient  $\chi$  and filter width  $\Delta$ . If  $\Phi$  is a linear map, the convergence of (10) towards the steady-state of (1) is guaranteed if all the eigenvalue magnitudes of this system are strictly smaller than one. Such a system is said to be (linearly) stable. As (10) depends on  $\chi$  and  $\Delta$ , these parameters play a key role in the stability of the SFD method. In the next section, we analyse this role, using a one-dimensional model.

### III. SCALAR PROBLEM

In this section a simple one-dimensional problem is studied in order to analyse the influence of  $\chi$  and  $\Delta$  on

the stability of the SFD method. A clear understanding of their role should help users of the SFD method to choose parameters that ensure its convergence. The scalar problem considered is

$$\dot{u} = \gamma u, \quad (11)$$

where  $\gamma \in \mathbb{C}$ . This equation has exact solver

$$u^{n+1} = \Phi_{1D}(u^n) = \alpha u^n, \quad \alpha = e^{\gamma \Delta t}. \quad (12)$$

For the remainder of this section we set  $\Delta t = 1$ .

The convergence towards the steady-state of (12) (*i. e.*  $u^{n+1} = u^n$ ) is guaranteed if  $|\alpha| < 1$ . We aim to use SFD to reach the steady-state of (12) when  $|\alpha| > 1$ . Analysing this simple case will allow us to highlight the roles of the parameters  $\chi$  and  $\Delta$  in the convergence (or not) of the SFD method.

In order to write the encapsulated formulation of the SFD method applied to (12), we use the function  $\Phi_{1D}$  such that  $\Phi_{1D}(u^n) = \alpha u^n$ . Then we introduce the operator  $\mathcal{L}_{1D}$  which has the same form as (7) upon replacing  $I$  with 1. The application of the encapsulated formulation of the SFD method to (12) becomes

$$\begin{pmatrix} u^{n+1} \\ \bar{u}^{n+1} \end{pmatrix} = e^{\mathcal{L}_{1D}} \begin{pmatrix} \alpha u^n \\ \bar{u}^n \end{pmatrix} = \underbrace{e^{\mathcal{L}_{1D}} \begin{pmatrix} \alpha & 0 \\ 0 & 1 \end{pmatrix}}_{M(\alpha, \chi, \Delta)} \begin{pmatrix} u^n \\ \bar{u}^n \end{pmatrix}, \quad (13)$$

where  $M$  is the iteration matrix transforming  $(u^n, \bar{u}^n)$  into  $(u^{n+1}, \bar{u}^{n+1})$  which depends on  $\alpha$ ,  $\chi$  and  $\Delta$ .

The eigenvalues (noted  $\lambda_1$  and  $\lambda_2$ ) of  $M$  can then easily be evaluated as functions of  $\alpha$ ,  $\chi$ , and  $\Delta$ . To ensure the stability of (13), we want to be able to choose  $\chi$  and  $\Delta$  such that  $\max(|\lambda_1|, |\lambda_2|) < 1$ .

From these eigenvalues we obtain the following limiting behaviour for small  $\chi$  and  $\Delta$ :

$$\begin{cases} \lim_{\chi \rightarrow 0} \lambda_1 = \alpha, \\ \lim_{\chi \rightarrow 0} \lambda_2 = e^{-1/\Delta}, \end{cases} \quad \begin{cases} \lim_{\Delta \rightarrow 0} \lambda_1 = \alpha, \\ \lim_{\Delta \rightarrow 0} \lambda_2 = 0. \end{cases} \quad (14)$$

If the original problem is not converging, applying the SFD method and choosing a small control coefficient  $\chi$  will not drive the solution towards its steady-state. We also obtain the following large  $\chi$  and  $\Delta$  limits:

$$\begin{cases} \lim_{\chi \rightarrow +\infty} \lambda_1 = 1, \\ \lim_{\chi \rightarrow +\infty} \lambda_2 = 0, \end{cases} \quad \begin{cases} \lim_{\Delta \rightarrow +\infty} \lambda_1 = \alpha e^{-\chi}, \\ \lim_{\Delta \rightarrow +\infty} \lambda_2 = 1. \end{cases} \quad (15)$$

If the control coefficient  $\chi$  (or the filter width  $\Delta$ ) is chosen to be large, the encapsulated formulation of the SFD method is marginally stable. The steady-state can not be reached but the solution does not blow up.

We now examine the stability regions of the encapsulated formulations of the SFD method. The goal, for a given control coefficient and filter width, is to identify for which  $\alpha$  the one-dimensional problem will converge

towards its steady-state. This section is only focused on the influence of  $\chi$  and  $\Delta$ .

In the stability diagram in Figure 1, each point of the complex plane corresponds to the value of  $\alpha$ . The values of  $\chi$  and  $\Delta$  are fixed for every point, and the eigenvalues of the iteration matrix  $M$  (define in Eq. (13)) are evaluated. If both eigenvalue magnitudes are smaller than one, then the point is coloured in grey. Hence the grey area corresponds to the stability region of (13). In other words, Figure 1(a) tells us that  $\chi = 1$  and  $\Delta = 0.5$  will drive (13) towards its steady-state for every  $\alpha$  chosen within the grey area.

We recall that (12) was stable only if  $|\alpha| < 1$  (*i. e.* only if  $\alpha$  was situated within the unit disc, delimited by the white circle on Figure 1). The stability region of (13) expands beyond the unit disc. These pictures allow us to visualize the fact that the SFD method stabilizes unstable modes. This is achieved without introducing a loss of stability elsewhere, indeed the stability region of the original problem (*i. e.* the unit disc) is inside the stability region.

On each stability diagram presented in Figure 1, we notice that if  $\alpha$  is real and greater than one, it is not possible to find a couple  $\chi$  and  $\Delta$  for which (13) is stable. Such an  $\alpha$  corresponds to a problem with a pure exponential growth of the instability. Hence we can conclude that the stability of the SFD method relies on the oscillatory growth of the problem studied. This is because time averaging oscillatory growth produces a good estimate of the equilibrium, whilst time averaging exponential growth does not. This was reported by Vyazmina<sup>7</sup>, who said that if an unstable eigenvalue is real and positive, there is no frequency to be damped by the SFD method.

Figure 1 presents stability regions for a fixed value of the control coefficient  $\chi$ . With a different  $\chi$ , the shape of these stability regions would have been similar but the area covered would have been different. This behaviour is shown in Figure 2.

Åkervik *et al.*<sup>2</sup> stated that choosing a large  $\chi$  or a large  $\Delta$  would make the system evolution very slow but the SFD method would eventually converge to a steady-state. The results presented in Figure 2 suggest that this may not always be true. Indeed, this picture shows that there is a region where (13) is stable for  $\chi = 0.5$  and  $\Delta = 20$  but unstable for  $\chi = 1$  and  $\Delta = 20$ . Hence increasing the control coefficient is not always an appropriate method to guarantee the convergence of the SFD method towards the steady-state.

When choosing a large filter width, the behaviour of the SFD method is slightly different. For a given  $\chi$  and a large  $\Delta$ , if the SFD method is not stable then it is not possible to find a smaller  $\Delta$  for which the method is stable. This is illustrated by the fact that the regions presented in Figures 1(a), 1(b) and 1(c) are all included within the region presented in Figure 1(d). However, choosing a very large  $\Delta$  does not guarantee the stability of (13). If  $\alpha$  is situated at the right of the unit circle,

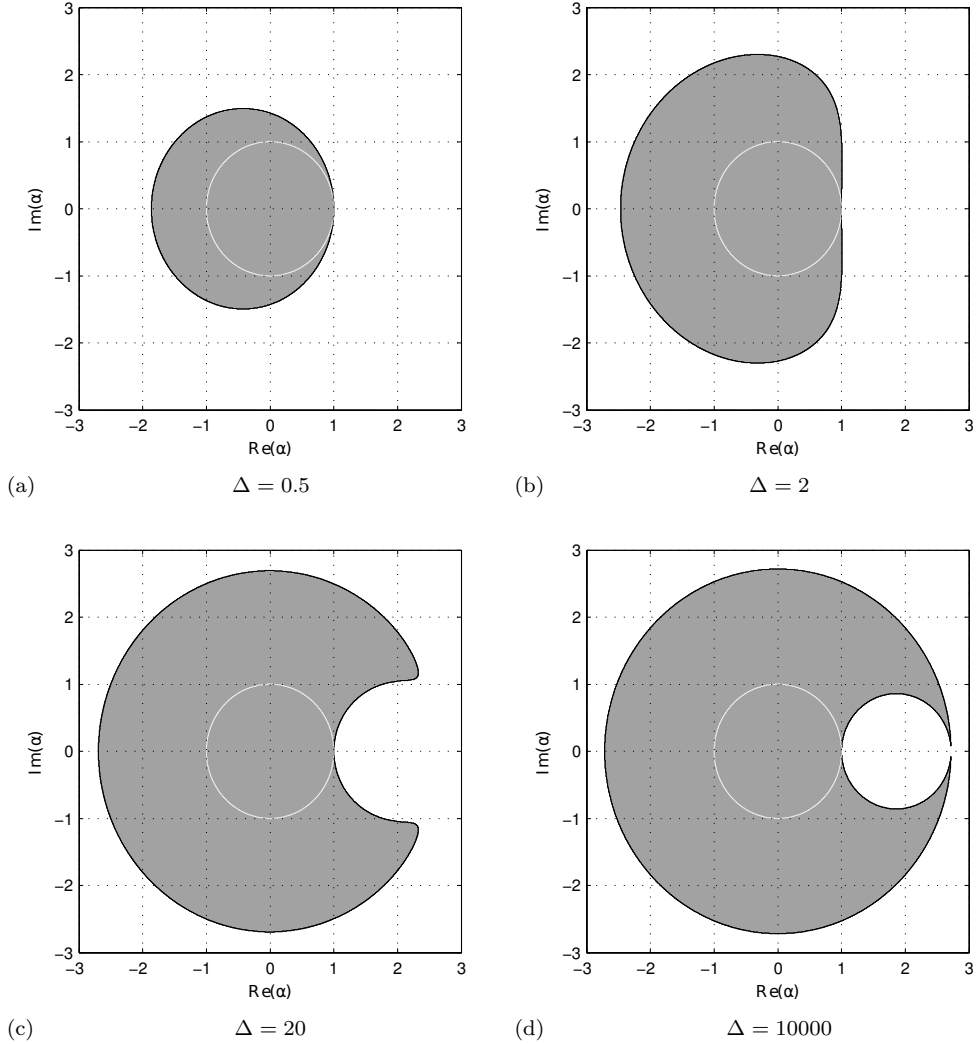


FIG. 1. Stability regions for  $\chi = 1$  and various  $\Delta$ . If  $\alpha$  is inside the grey area then (13) converges towards the steady-state of (12). The unit circle (*i. e.* the region where  $|\alpha| = 1$ ) is displayed in white.

close to the real axis, increasing the filter without acting on the control coefficient might not be enough to enable the SFD method to converge.

When  $\chi = 0$  and when  $\Delta$  tends to zero, the stability region of (13) fits exactly within the unit circle, confirming the outcome of the limiting behaviour analysis for the scalar problem (for conciseness these figures are not presented here).

Note that a second order Strang splitting method<sup>12</sup> can also be used to solve (5) applied to the scalar problem (12). The procedure would be to solve the subproblem (7) on half a time-step, then to apply the solver  $\Phi$  on a whole time step and finally to solve (7) again on half a time step. The stability regions obtained using this method are exactly the same as the ones presented in this section. This is because the second-order splitting can be written as a shifted first-order splitting with a pre- and post-processing step, so both methods have the

same stability regions.

#### IV. NUMERICAL EXPERIMENTS

In this section we present the numerical steady-state of the two-dimensional incompressible flow past a cylinder above its critical Reynolds number  $Re_c$ . At  $Re = 100$  this flow is unstable and von Kármán vortex streets are observable. Indeed, shedding vortices appear when the Reynolds number is high enough such that the viscous forces within the flow are not dominant (*i. e.*  $Re > Re_c \simeq 47$ ). This phenomenon remains until the end of the subcritical regime ( $Re \simeq 2 \times 10^5$ )<sup>13</sup>. Hence the goal of the SFD method is to suppress these oscillations and drive the solution towards its steady-state.

The problem dimensions are  $-15 \leq x \leq 45$  and  $-25 \leq y \leq 25$ . The cylinder is centred at the origin

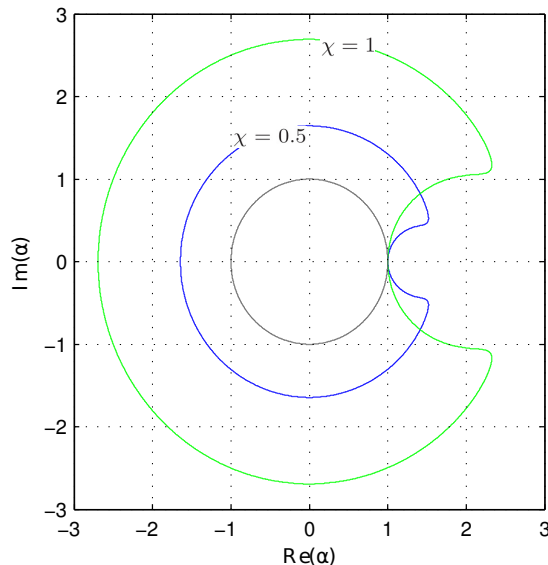


FIG. 2. Contours of the stability regions of (13) for  $\Delta = 20$  and two different  $\chi$ . The central circle represents the boundary of the unit disc.

and its diameter is one unit length. On the cylinder surface, no-slip boundary conditions are imposed. Dirichlet boundary conditions  $(u, v) = (1, 0)$  are imposed on the left, top and bottom edges. Finally an outflow boundary condition is set on the right edge.

To find the steady-state solution of the two-dimensional cylinder flow problem at  $Re = 100$ , we implemented the encapsulated SFD method (10) into the Nektar++ spectral/ $hp$  element framework<sup>14</sup>, as a wrapper function. In order to find the steady-state solution of the incompressible Navier-Stokes equations, a solver which implements the *velocity-correction* scheme<sup>15</sup> (which defines  $\Phi$  in (10) in this case) is called at each time-step.

The computational domain is composed of 746 elements, with structured quadrilaterals close to the cylinder boundary and triangles elsewhere. An unstabilised continuous Galerkin method<sup>15</sup> is used to discretize the problem in space; and the time-integration scheme used is a second order IMEX method<sup>16</sup>.

As the steady solution is expected to be smooth, a high polynomial order of 11 is used. To highlight the fact that, in contrast to Newton's methods, the SFD method does not need a good approximation of the final solution to converge, initial conditions such as  $(u_0, v_0) = (0, 0)$  are chosen. The SFD parameters are initially chosen such that the control coefficient  $\chi = 1$  and the filter width  $\Delta = 2$ . The problem is considered to have converged when  $\|q^n - \bar{q}^n\|_{\inf} < 10^{-8}$ . The steady-state has been obtained after the computation of about 1000 time units (with the time-step  $\Delta t = 0.01$ ) and the decay of  $\|q^n - \bar{q}^n\|_{\inf}$  is exponential.

Figure 3(a) is simply a reminder of the behaviour of

the uncontrolled incompressible cylinder flow at  $Re = 100$  and the steady-state obtained by SFD is shown on Figure 3(b). This flow configuration is identical to the one presented by Barkley<sup>1</sup>.

A stability analysis, using an Arnoldi method, is performed with this steady-state as the "base flow". The growth rate  $\sigma$  and the frequency  $f$  of this flow configuration are

$$\sigma = 0.12978 \quad \text{and} \quad f = 2\pi \times 0.11769, \quad (16)$$

which correspond to the values presented by Barkley<sup>1</sup>. If the time length of each Arnoldi iteration is defined as being equal to one time unit, this growth rate and this frequency correspond to the two dominant (conjugate) eigenvalues

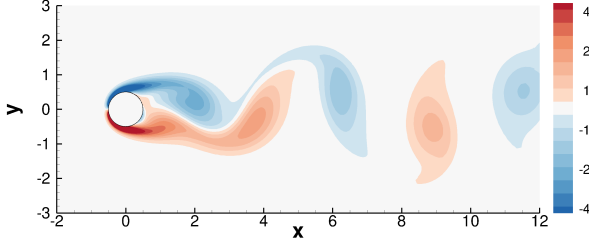
$$\lambda_{1,2} = 1.13857e^{\pm 0.73944i}. \quad (17)$$

As  $|\lambda_{1,2}| > 1$ , the flow is unstable and the corresponding instabilities exponentially grow through time. However the SFD method was able to stabilise the flow and allowed it to converge towards its steady-state.

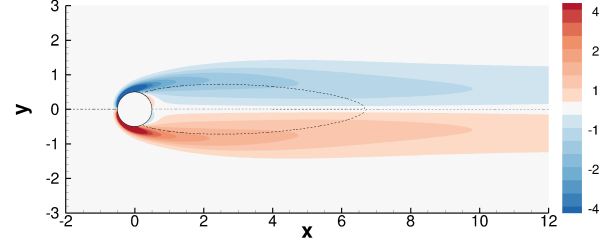
We conducted a numerical experiment to verify that the results of the 1D analysis are relevant to nonlinear SFD. First, we obtained the dominant eigenvalues (noted  $\lambda_D$ ) of the steady-state cylinder flow. By analysing the stability of the scalar problem (13), we were able to obtain a control coefficient  $\chi_D$  and a filter width  $\Delta_D$  which enable to reach the steady-state of  $u^{n+1} = \lambda_D u^n$  when applied to the 1D problem, using our analysis. We then verified that these parameters also ensure convergence of the SFD method applied to the flow problem.

Figure 4 shows the contours of several stability regions of (13), superposed with the position of the dominant (conjugate) eigenvalues (17) of the cylinder flow at  $Re = 100$ . (Note that the stability regions of  $\chi = 1$ ,  $\Delta = 0.5$  and  $\chi = 1$ ,  $\Delta = 2$  are the ones shown on Figure 1(a) and 1(b)). We notice that for  $\chi = 1$  and  $\Delta = 1$  and also for  $\chi = 1$  and  $\Delta = 2$ , the unstable eigenvalues (17) are situated inside the stability region of (13). These parameter couples have been used to apply the SFD method to the Navier-Stokes solver and with both, the steady solution was obtained. However the computational time required to reach convergence strongly depends  $\chi$  and  $\Delta$ . Figure 5(a) compares the number of iterations computed by the Navier-Stokes solver before obtaining the steady-state. With  $\chi = 1$  and  $\Delta = 1$  the SFD method needs about 4 times as many iterations to converge than with  $\chi = 1$  and  $\Delta = 2$ . Increasing the filter width does not always decrease the computation time of the method. Indeed when  $\Delta$  becomes too large, we obtain the expected limiting behaviour.

For  $\chi = 1$  and  $\Delta = 0.5$ , the unstable eigenvalues (17) are situated outside the stability region of (13). When this parameter couple is used to apply the SFD method to the cylinder flow, the steady-state can not be obtained. Figure 6 presents the outcome of the method with



(a) Snapshot of the uncontrolled flow (unsteady and periodic). This behaviour is the well known von Kármán shedding.



(b) Unstable steady-state obtained by SFD. The dashed lines represent the separating streamlines.

FIG. 3. Vorticity ( $\omega = \partial_x v - \partial_y u$ ) of the incompressible flow past a two-dimensional cylinder at  $Re = 100$ . Note that only a small part of the whole computational domain is displayed.

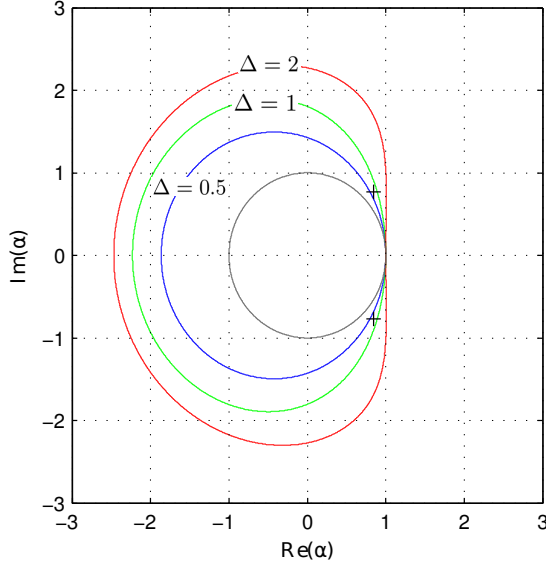


FIG. 4. Contours of the stability regions of (13) for  $\chi = 1$  and various  $\Delta$ . The central circle represents the boundary of the unit disc. The two black crosses indicate the position of the dominant unstable eigenvalues (17) of the cylinder flow at  $Re = 100$ .

these parameters. This flow is not steady but the oscillations are attenuated in comparison with the flow presented in Figure 3(a). Figure 5(b) shows that when the SFD method is not converging towards a steady-state,  $\|q - \bar{q}\|_{\inf}$  does not decrease but it oscillates around a fixed value.

In summary we can say that a relationship can be drawn between the convergence (or not) of the SFD method applied to (12) with  $\alpha = \lambda_D$  and the ability of the SFD to drive the flow problem towards its steady-state. Note that the problem studied here has only two (conjugate) unstable eigenmodes.

We also substitute  $\alpha = \lambda_D$  in the iteration matrix  $M$  (define in Eq. (13)) and numerically optimized the eigenvalues of this operator (*i. e.* we minimized the amplitude

of the largest eigenvalue) by adjusting the values of the control coefficient and the filter width. We obtained optimum parameters  $\chi_{\text{opt}} \simeq 0.4391$  and  $\Delta_{\text{opt}} \simeq 3.1974$ . We observed that these parameters gave the fastest SFD convergence when applied to the cylinder flow (about 15% faster than for  $\chi = 1$  and  $\Delta = 2$ ). The convergence history of this case is shown on Figure 5(a).

## V. IMPLICIT METHODS FOR SFD

It is useful to make a comparison between the encapsulated SFD method with explicit coupling and a fully implicit discretisation of the time-continuous SFD equations (5). In this case, the formulation is not encapsulated any more, and an implicit solver requires modification to include the SFD terms. In particular, this doubles the dimension of the implicit problem. We performed a 1D analysis of the backward Euler scheme applied to (5), in the case  $f(q) = \gamma q$ , with  $\exp(\gamma \Delta t) = \alpha$ . We found the following conclusions. First, in the case  $\chi = 0$  (in which case the system reverts to the uncontrolled system (1)), the map is stable for all eigenvalues  $\alpha$ , except for a circular bubble to the right of  $\alpha = 1$  (see Figure 7). This means that it is possible to stabilise pure exponential growth for sufficiently large growth factor. Second, when  $\chi$  increases (and  $\chi > 0$ ), the size of this bubble region increases, and so SFD actually makes the scheme *less stable*. Third,  $\Delta$  does not substantially affect the shape of the unstable region, but does accelerate the convergence to steady-state for small  $\Delta$ . This means that SFD can be used to accelerate convergence to steady-state if backward Euler is already stable for a given value of  $\alpha$ .

## VI. CONCLUSION

An alternative formulation of the SFD method, which enables us to use an already existing time-stepping code as a "black box", is presented. This method can be easily implemented as a wrapper function. The convergence towards the unstable steady-state of the two-dimensional incompressible flow past a cylinder at  $Re = 100$  is

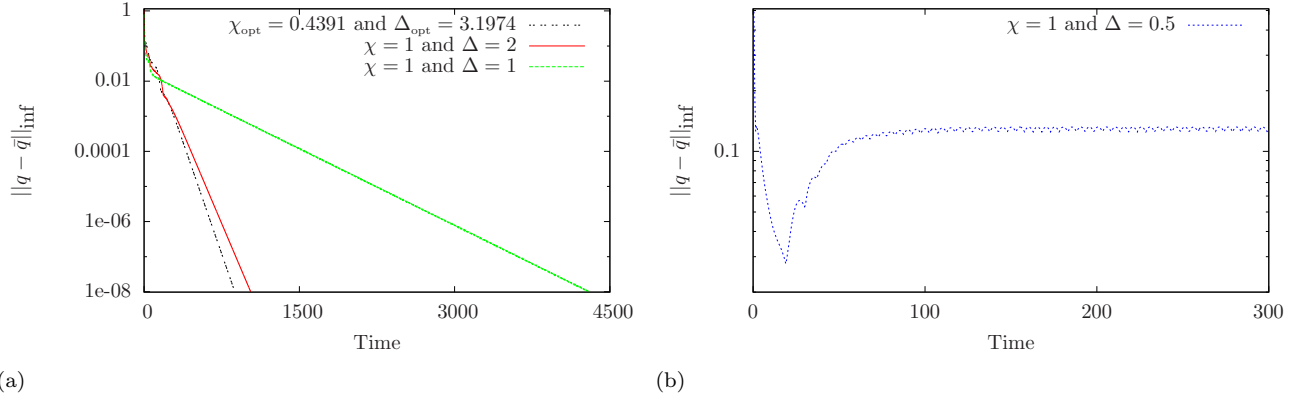


FIG. 5. Time evolution of  $\|q - \bar{q}\|_{\text{inf}}$  for parameters which allow the encapsulated SFD method to converge towards the steady-state of the incompressible flow past a two-dimensional cylinder at  $Re = 100$  (a); and for parameters which do not (b). The cases presented here have been computed with the time-step  $\Delta t = 0.01$ .

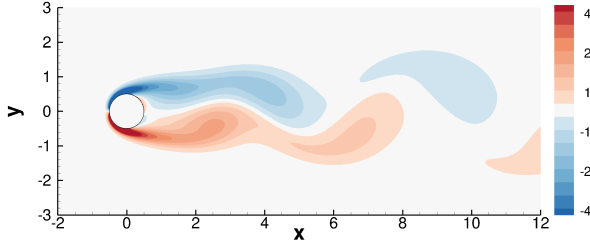


FIG. 6. Vorticity of the partially controlled flow cylinder flow at  $Re = 100$ . Snapshot obtained with SFD parameters which do not allow convergence towards the steady-state.

achieved without the use of a continuation method, and the result matches with that of Barkley<sup>1</sup>.

The stability of the method relies on the oscillatory growth of the problem studied. Indeed a problem which has a pure exponential growth corresponds to a case where the dominant unstable eigenvalue would be real. We have observed that the encapsulated SFD method is not able to find the steady-state of such cases (*e. g.* wall confined jets<sup>17</sup>). We also studied implicit methods for SFD, and found that SFD can not improve the stability region compared with backward Euler applied to the uncontrolled system, but can increase the rate of convergence to a steady-state.

If the problem has unstable eigenvalues with an imaginary part, the convergence towards the steady-state relies upon an appropriate choice of the parameters  $\chi$  and  $\Delta$ . The knowledge of the dominant eigenvalue  $\lambda_D$  of the system allows us to select suitable parameters through the analysis of the stability of the SFD method applied to  $u^{n+1} = \lambda_D u^n$ . However most of the time the dominant eigenvalue of a challenging flow problem is not known *a priori*. This suggests to investigate the possibility of coupling the SFD method with an Arnoldi method which would evaluate the dominant eigenvalue using a "partial" steady-state for base flow (*e. g.* the solution when

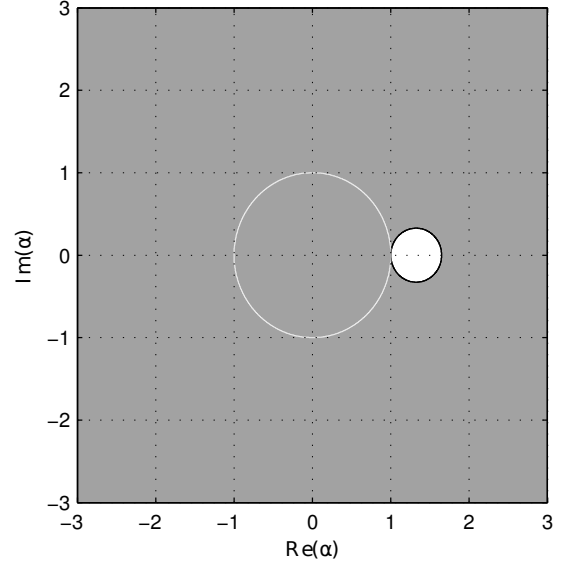


FIG. 7. Stability region of a fully implicit discretisation of the time-continuous SFD equations (5) in the 1D case  $f(q) = \gamma q$  (with  $\exp(\gamma \Delta t) = \alpha$  and  $\Delta t = 0.25$ ) and  $\chi = 0$ . If  $\alpha$  is inside the grey area then the scheme is stable and the steady-state can be found. The unit circle (*i. e.* the region where  $|\alpha| = 1$ ) is displayed in white.

$\|q^n - \bar{q}^n\|_{\text{inf}} \simeq 10^{-2}$ ). The idea would be to obtain an approximation of the dominant eigenvalue in order to be able to choose appropriate  $\chi$  and  $\Delta$ .

## ACKNOWLEDGMENTS

The authors would like to thank the Seventh Framework Programme of the European Commission for their support to the ANADE project (Advances in Numerical



and Analytical tools for DETached flow prediction) under grant contract PITN-GA-289428.

- <sup>1</sup>D. Barkley. Linear analysis of the cylinder wake mean flow. *EPL (Europhysics Letters)*, 75(12):750, 2006.
- <sup>2</sup>E. Åkervik, L. Brandt, D. S. Henningson, J. Hoepffner, O. Marxen, and P. Schlatter. Steady solutions of the Navier-Stokes equations by selective frequency damping. *Phys. Fluids*, 18, 2006.
- <sup>3</sup>B. Pier. Local and global instabilities in the wake of a sphere. *J. Fluid Mech.*, 603:39–61, 2008.
- <sup>4</sup>S. Bagheri, P. Schlatter, P. J. Schmid, and D. S. Henningson. Global instability of a jet in crossflow. *Phys. Fluids*, 18:028104, 2006.
- <sup>5</sup>E. Åkervik, J. Hoepffner, U. Ehrenstein, and D. S. Henningson. Optimal growth, model reduction and control in a separated boundary-layer flow using global eigenmodes. *J. Fluid Mech.*, 579(1):305–314, 2007.
- <sup>6</sup>L. E. Jones and R. D. Sandberg. Numerical analysis of tonal airfoil self-noise and acoustic feedback-loops. *J. Sound Vib.*, 330(25):6137–6152, 2011.
- <sup>7</sup>E. Vyazmina. *Bifurcations in a swirling flow*. PhD thesis, École Polytechnique, 2010.
- <sup>8</sup>J. Kim and T. R. Bewley. A linear systems approach to flow control. *Annu. Rev. Fluid Mech.*, 39:383–417, 2007.
- <sup>9</sup>C. D. Pruett, T. B. Gatski, C. E. Grosch, and W. D. Thacker. The temporally filtered Navier-Stokes equations: Properties of the residual stress. *Phys. Fluids*, 15(8):2127, 2003.
- <sup>10</sup>C. D. Pruett, B. C. Thomas, C. E. Grosch, and T. B. Gatski. A temporal approximate deconvolution model for large-eddy simulation. *Phys. Fluids*, 18:028104, 2006.
- <sup>11</sup>L. S. Tuckerman and D. Barkley. *Bifurcation analysis for timesteppers*. Springer, 2000.
- <sup>12</sup>I. Faragó. Splitting methods and their application to the abstract Cauchy problems. In *Numerical Analysis and Its Applications*, pages 35–45. Springer, 2005.
- <sup>13</sup>C. Norberg. Fluctuating lift on a circular cylinder: review and new measurements. *J. Fluids Struct.*, 17:57–96, 2003.
- <sup>14</sup>Nektar++. <http://www.nektar.info>, 2013.
- <sup>15</sup>G. E. Karniadakis and S. J. Sherwin. *Spectral/hp Element Methods for CFD*. Oxford University Press, second edition, 2005.
- <sup>16</sup>U. M. Ascher, S. J. Ruuth, and B. T. R. Wetton. Implicit-explicit methods for time-dependent partial differential equations. *SIAM J. Numer. Anal.*, 32(3):797–823, 1995.
- <sup>17</sup>S. J. Sherwin and H. M. Blackburn. Three-dimensional instabilities and transition of steady and pulsatile axisymmetric stenotic flows. *J. Fluid Mech.*, 533:297–327, 2005.